PHILOSOPHICAL TRANSACTIONS OF THE ROYAL SOCIETY A MATHEMATICAL, PHYSICAL & ENGINEERING SCIENCES

New light on electron––ion collisions from heavy–ion storage ring experiments

The Royal Society

Phil. Trans. R. Soc. Lond. A 1999 **357**, 1279-1296
doi: 10.1098/rsta.1999.0374

THE ROYAL SOCIETY

New light on electron–ion collisions from heavy-ion storage ring experiments

By Alfred Müller

Institut für Kernphysik, Strahlenzentrum der Justus-Liebig-Universität Giessen, Leihgesterner Weg 217, D-35392 Giessen, Germany

Experiments with merged beams of electrons and ions stored in accelerator rings have provided a wealth of new data on electron–ion collision processes. The development towards lower and lower temperatures of electron beams and the availability of brilliant beams of ions up to the highest charge states has opened up a precision atomic spectroscopy through the observation of resonances. The available technology also provides unique new access to very low electron–ion collision energies. There, typically below a few millielectronvolts, an unexpected enhancement is observed in the recombination of atomic ions with electrons. For U^{28+} ions, where such enhancement was seen for the first time, the measured rate coefficient is roughly a factor of 200 higher than expectation for radiative recombination. The experimental spectrum can be simulated by assuming dielectronic recombination (DR) resonances at very low energies. However, recombination enhancements are also observed with completely stripped ions where no DR resonances can occur. Systematic studies of dependences of the new phenomenon on ion charge state, electron density and temperature, and on external electromagnetic fields are being carried out. So far, however, a satisfactory understanding is still missing.

Keywords: ionization; recombination; rate enhancement; field effects; interference; spectroscopy

1. Introduction

Electron–ion collisions are important fundamental processes in all plasmas. They determine the charge-state balance of the ions and, hence, also the spectrum of electromagnetic radiation emitted by the plasma. Understanding and diagnosing the state of a plasma, whether of astrophysical origin or man-made, relies on information about cross-sections and rate coefficients for electron–ion interactions.

Interacting beams of electrons and ions (Brouillard 1986) have been used for almost 40 years in experimental studies of electron–ion collision processes. By the combination of the well-known merged-beams approach with ion accelerator technology, a new era of electron–ion collision studies began a little over a decade ago (Graham *et al*. 1992). By merging bright cooled beams of swift ions with very cold intense and well-characterized electron beams, energies in the electron–ion centre-of-mass frame from zero to several kiloelectronvolts are accessible. Energy spreads as low as *ca.* 10 meV have been experimentally verified at low energies. Intense beams of almost any species of atomic ions can presently be made available, depending on the choice of accelerator facility. These new opportunities have been used to study electron-impact ionization and recombination of many ions from Li^{+} to U^{89+} (Müller 1995).

The objectives of research have been manifold. A large fraction of the experiments has addressed issues of a fundamental nature. Hence, measurements were carried out for ions with only few core electrons, where theoretical techniques can be sensitively tested. These studies involve recombination of completely stripped ions with electrons, interactions with ions carrying one, two or three core electrons, and collisions of ions with only one active electron outside closed shells, such as Na-like Fe^{15+} (Linkemann *et al.* 1995*a*, *b*). However, the applied aspects of electron–ion collisions for plasma and accelerator physics also led to efforts to study systems with more complex electronic structures. Among these are fluorine-like Se^{25+} (Lampert *et al.* 1996) and Fe^{17+} (Savin *et al.* 1997). While the first of these ions is important in connection with the attempts to develop short-wavelength lasers, the latter is relevant to the understanding of the radiation spectrum from astrophysical plasmas. An experimental programme at the Heidelberg test storage ring (TSR) aims at providing collision cross-sections and rate coefficients of the astrophysically abundant Fe^{q+} ions with $q = 15, 16, \ldots, 23$. Measurements are also becoming available for many-electron ions such as U^{28+} (Uwira *et al.* 1995; Mitnik *et al.* 1998), Au^{25+} (Hoffknecht *et al.* 1998) or Au^{50+} (Uwira *et al.* 1997*a*). There, the primary goal of experiments is the understanding of the observation of unexpected huge recombination rates of such ions at low relative energies, i.e. under electron-cooling conditions. Recombination losses of ions during the preparation of intense ion beams in storage rings has become a serious issue in accelerator physics (Baird *et al.* 1995). The fortuitous presence of dielectronic recombination (DR) resonances near zero energy on top of the omnipresent radiative recombination (RR), appears to explain the observed hugely enhanced recombination rates to some (large) extent. However, the studies that have been carried out so far also indicate effects of the strongly coupled cold plasmas envisaged during ion cooling in the electron beam of the cooling device. Such effects are also studied with completely stripped primary ions (Gao *et al.* 1995; Uwira *et al.* 1996), where the atomic structure cannot support resonances, and where, nevertheless, recombination rate enhancements up to factors of *ca.* 10 have also been observed (see, for example, Uwira *et al.* 1997*b*).

The following major issues have been addressed in electron–ion collision studies at storage rings:

(i) accurate rates and cross-sections for ionization and recombination;

(ii) spectroscopy of doubly excited states by the observation of resonances;

(iii) field effects on recombination rates;

(iv) clarification of observed recombination rate enhancements at low energies;

(v) interference phenomena particularly in the recombination channel; and

(vi) indirect ionization mechanisms for ions of intermediate high charge states.

Examples of recent investigations related to some of these topics are presented below.

2. Experimental features

(*a*) *The measurements*

For the measurement of rates and cross-sections, ions of the desired species are injected into a storage ring from an accelerator. High beam currents (up to the mA

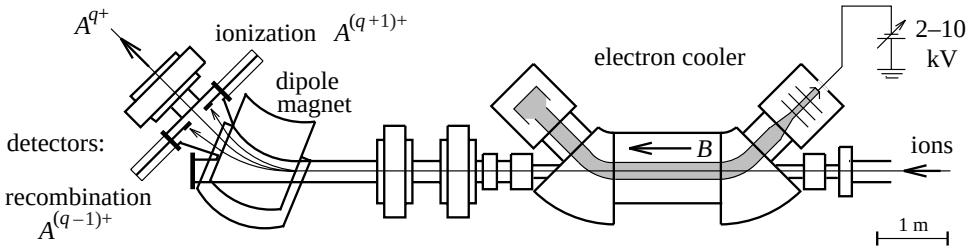

Figure 1. Schematic of the cooler section of a storage ring (in this case the Heidelberg TSR). The ion beam circulating in the ring is merged with the electron beam (shaded) of the electron cooler. Products of charge-changing collisions, i.e. ionized $A^{(q+1)+}$ and recombined $A^{(q-1)+}$ ions are separated from the beam of circulating A^{q+} ions by the dipole magnet behind the cooler and detected on the 'inside' and 'outside' of the ring, respectively.

range depending on ion species and injector) can be accumulated, and the ions are cooled by friction forces in the electron beam of the cooling device. So far, this beam has had to serve both for the cooling of ion beams and as an electron target for collision experiments.

When the ion beam is sufficiently cold, the energy of the electron beam is detuned from 'cooling' and, accordingly, the relative energy between the ion and electron beams is increased from zero. In collisions with the electrons of the cooler, stored ions change their original charge state and, by doing so, they drop out of the ring and can be detected without disturbing the circulating ion beam. Suitable particle detectors are mounted both at the outer and the inner side of the ring, typically behind the first beam-bending magnet downbeam from the electron cooling device (see figure 1), so as to facilitate collection of recombined and ionized product ions, respectively. Counting rates R_{exp} are recorded as a function of the electron energy, which is rapidly scanned over a certain range, usually in small steps with intermittent beam cooling after each voltage step. Scans are repeated until the desired level of statistics is reached.

(*b*) *Rate coefficients*

Normalized collision rates (rate coefficients) α are determined from the relation

$$\alpha(E_{\mathrm{rel}}) = \frac{R_{\mathrm{exp}}\gamma^2 v_{\mathrm{i}} qe}{I_{\mathrm{i}}\ell_{\mathrm{eff}} n_{\mathrm{e}}\varepsilon}. \tag{2.1}$$

Detection efficiencies ε of the particle detectors are usually close to 1, I_{i} is the measured electrical current of the circulating ion beam, v_{i} the ion velocity, qe the ion charge, ℓ_{eff} the interaction length of the two beams, n_{e} the electron density, and $\gamma = \gamma(v_{\mathrm{i}})$ is the relativistic Lorentz factor for the ion beam in the laboratory frame. Statistical uncertainties in the measured data can, in most cases, be reduced to insignificance, total systematic uncertainties are typically of the order of $\pm 20\%$.

The rates α basically depend on the velocity spread within the electron beam and the collision cross-section σ:

$$\alpha(v_{\mathrm{rel}}) = \langle \sigma v_{\mathrm{rel}} \rangle = \int \sigma(v) v f(v_{\mathrm{rel}}, \boldsymbol{v})\, \mathrm{d}^3 v. \tag{2.2}$$

For the particular case of merged electron and ion beams in storage cooler rings, two velocity coordinates are commonly used to describe the electron-velocity distribu-

tion in the rest frame of the ions: $v_{\|}$, the velocity component in electron-beam direction; and $v_{\perp}$, the velocity component perpendicular to the electron-beam direction. The energy (or velocity) spreads are, therefore, characterized by two corresponding temperatures: $T_{\|}$ for the longitudinal; and $T_{\perp}$ for the transverse direction. In the accelerated electron beam, these temperatures are quite different, with $T_{\|} \ll T_{\perp}$, so that $f(\boldsymbol{v})$ is highly anisotropic. Its mathematical form is given by

$$f(v_{\mathrm{rel}}, \boldsymbol{v}) = \frac{m_{\mathrm{e}}}{2\pi k T_{\perp}} \exp\left(-\frac{m_{\mathrm{e}} v_{\perp}^2}{2kT_{\perp}}\right) \sqrt{\frac{m_{\mathrm{e}}}{2\pi k T_{\|}}} \exp\left(-\frac{m_{\mathrm{e}}(v_{\|} - v_{\mathrm{rel}})^2}{2kT_{\|}}\right), \tag{2.3}$$

where m_{e} denotes the electron rest mass. The quantity v_{rel} in this formula is the average longitudinal centre-of-mass velocity

$$v_{\mathrm{rel}} = \frac{|v_{\mathrm{e},\|} - v_{\mathrm{i},\|}|}{1 + [(v_{\mathrm{i},\|} v_{\mathrm{e},\|})/c^2]}, \tag{2.4}$$

where c is the vacuum speed of light, and where $v_{\mathrm{e},\|}$ and $v_{\mathrm{i},\|}$ are the longitudinal velocity components of the electron and ion beams in the laboratory frame, respectively. They are determined from

$$v_{e/i,\|} = c\sqrt{1 - \left[1 + \frac{E_{\mathrm{e/i}}}{m_{\mathrm{e/i}} c^2}\right]^{-2}}. \tag{2.5}$$

The ion rest mass is m_{i}. The energies E_{e} and E_{i} are determined by electron and ion acceleration voltages, respectively. The relative velocity v_{rel}, as defined by equation (2.4), can be different from the velocity v_{cm} in the electron–ion centre-of-mass frame. This is especially true for low energies, where E_{cm} comes close to $kT_{\perp}$ and $kT_{\|}$. Since only E_{rel} is directly accessible to measurement, experimental data are usually displayed as a function of the relative energy

$$E_{\mathrm{rel}} = (\gamma_{\mathrm{rel}} - 1) m_{\mathrm{e}} c^2, \tag{2.6}$$

with

$$\gamma_{\mathrm{rel}} = [1 - (v_{\mathrm{rel}}/c)^2]^{-1/2}. \tag{2.7}$$

(c) *Energy resolution*

An important issue in most electron–ion collision experiments is the energy resolution. Cross-sections are often characterized by the presence of narrow features, such as excitation steps or sharp resonances. Resolving these features provides detailed insight into the physics behind the collision processes. The energy resolution of electron–ion merged-beams experiments at storage rings is mainly determined by the longitudinal and transverse temperatures of the electron beam. In the limit of vanishing $kT_{\|}$, the rate coefficient α of a narrow resonance is characterized by an asymmetric line profile with an exponential decrease towards lower relative energy, and a sharp cut-off at the resonance energy. The exponential function is determined by $kT_{\perp}$ and a full width at half maximum (FWHM) of

$$\Delta E_{\perp} = kT_{\perp} \ln 2 \tag{2.8}$$

for the distribution function. In the limit of infinitely small $kT_{\perp}$, the rate coefficient for a narrow resonance assumes a Gaussian shape with a FWHM of

$$\Delta E_{\|} = 4\sqrt{\ln 2 k T_{\|} E_{\mathrm{rel}}}. \tag{2.9}$$

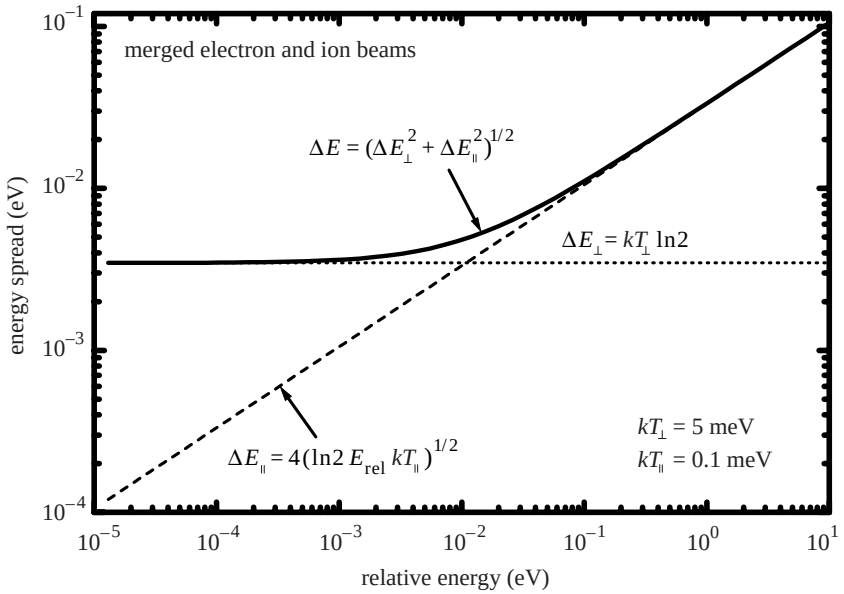

Figure 2. Energy spread (solid line) to be expected in a merged-beams electron–ion collision experiment at a storage ring as a function of the relative energy between the colliding particles for electron-beam temperatures $kT_\parallel = 0.1$ meV and $kT_\perp = 5$ meV. Partial energy spreads are also indicated.

The two values for the resonance width are of equal size at an energy

$$E_{\mathrm{eqs}} = \frac{\ln 2 (kT_\perp)^2}{16 kT_\parallel}. \tag{2.10}$$

At low relative energies with $E_{\mathrm{rel}} \ll E_{\mathrm{eqs}}$, the perpendicular temperature of the electron beam limits the energy resolution. Correspondingly, the parallel temperature determines the energy spread at high relative energies $E_{\mathrm{rel}} \gg E_{\mathrm{eqs}}$. In the general case with finite values of $kT_\perp$, $kT_\parallel$ and a resonance linewidth Γ, the total FWHM of the apparent cross-section (or the rate coefficient) is

$$\Delta E = \sqrt{(kT_\perp \ln 2)^2 + 16 \ln 2 kT_\parallel E_{\mathrm{rel}} + \Gamma^2}. \tag{2.11}$$

Since the first application of the merged-beams techniques to collision studies involving multiply charged ions, enormous progress has been made in reducing electron-beam temperatures. While in the pioneering experiments the electron beam was characterized by $kT_\perp \approx 5$ eV and $kT_\parallel \approx 60$ meV (see, for example, Dittner *et al.* 1987), the first storage ring cooler used in single-pass merged-beams experiments provided $kT_\perp \approx 0.15$ eV and $kT_\parallel \approx 2$ meV (see, for example, Andersen *et al.* 1990). The race for lower temperatures is going on and the present record is held by the cooler of CRYRING, where evidence has been found for $kT_\perp \approx 1$ meV and $kT_\parallel \approx 0.06$ meV (H. Danared, personal communication). The cooler of the TSR is only slightly behind, and a new electron target development in Heidelberg is promising to push the frontier to yet lower temperatures.

For a set of typical low temperatures $kT_\parallel = 0.1$ meV and $kT_\perp = 5$ meV in a merged-beams experiment, figure 2 shows the experimental energy spread over a

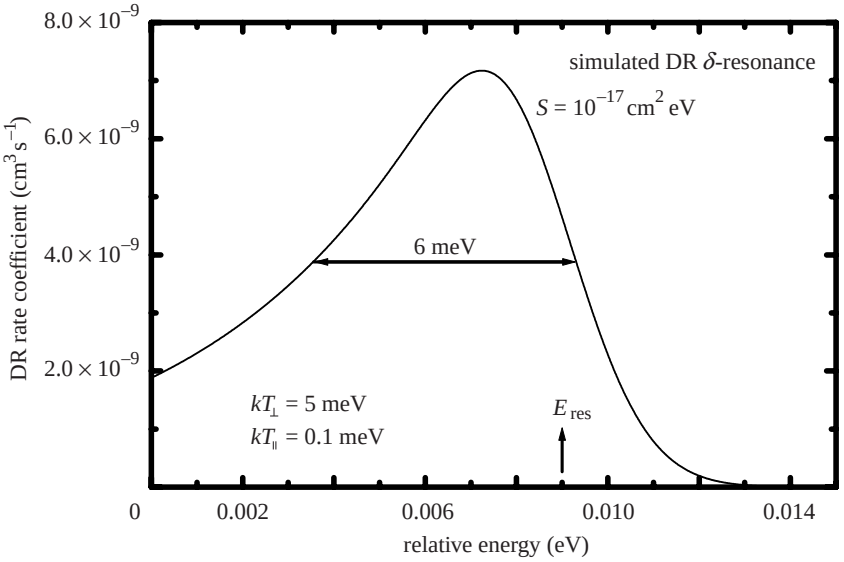

Figure 3. Simulated experimental dielectronic recombination resonance calculated by convolution of a δ-function (according to equations (2.2) and (2.3)). The δ-resonance is assumed to be at $E_{\mathrm{res}} = 9$ meV, with a resonance strength $S = \int \sigma(E)\,\mathrm{d}E = 10^{-17}$ cm^2 eV.

wide range of relative energies. According to equation (2.10), the energy where parallel and transverse energy spreads match is expected at 10.8 meV, in accordance with the figure. Using the same electron-beam temperatures, the experimental profile of a δ-resonance situated at $E_{\mathrm{res}} = 9$ meV was simulated by using the above equations. The line profile is shown in figure 3. It is clearly asymmetric as predicted for $E_{\mathrm{rel}} \leqslant E_{\mathrm{eqs}}$, and its width is predominantly determined by $kT_{\perp}$. The observed peak is only 6 meV wide.

The consequence of the ongoing technical development towards lower electron-beam temperatures becomes obvious in figure 4, where the results of three measurements of DR of C^{3+} ions are displayed. Identical scales have been applied to each display box. The differences in energy resolution need no further comment, nor does the accessibility of very low relative energies. Truncation of the Rydberg state population is different in the three experiments and so is the influence of external electromagnetic fields. Hence, the areas under the different curves cannot be directly compared to each other. In a recent publication, Mannervik *et al.* (1998) present a CRYRING measurement of the resonance group displayed in the inset of figure 4. Their energy resolution in that experiment is comparable to the result of G. Gwinner (personal communication) that was measured at the TSR.

3. Measurements and results

(*a*) *Ionization*

Few experiments have been carried out at storage rings on electron-impact ionization of ions. The measurements have been restricted, so far, to net single ionization. The great advantage of storage rings for such work is, firstly, in the accessibility of sufficiently intense beams of highly charged ions and, secondly, in the potential

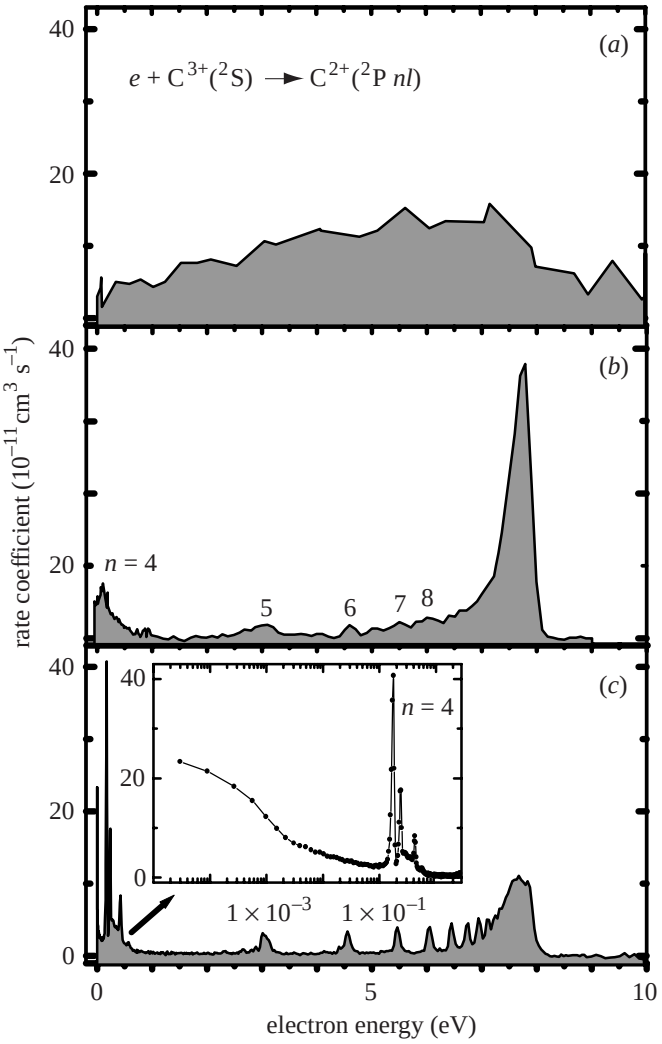

Figure 4. Comparison of three measurements of DR of C^{3+} ions. The resonance features are due to transitions $e + C^{3+}(1s^2 2s) \rightarrow C^{2+}(1s^2 2p n\ell) \rightarrow C^{2+}(1s^2 2s^2) +$ photons. In the experiments, different external electromagnetic fields and different levels of field ionization were involved. The data are from the work of (*a*) Dittner *et al*. (1987), (*b*) Andersen *et al*. (1990) and (*c*) G. Gwinner (personal communication). The results show the development of energy resolution in such experiments over a time span of a little over 10 years. The TSR data in (*c*) are preliminary.

of handling metastable beam components. The storage of the ions for a sufficiently long time to make excited states decay before starting a measurement provides well-defined ground-state ion beams. On the other hand, storage lifetimes and ion charge states are closely related to the ion energy, which is generally so high that electron stripping in the residual gas of the ring produces very substantial background in the detector for ionized product ions. Thus, electron-impact ionization may provide only a few percent of the total counting rate of ionized and stripped ions. Neverthe-

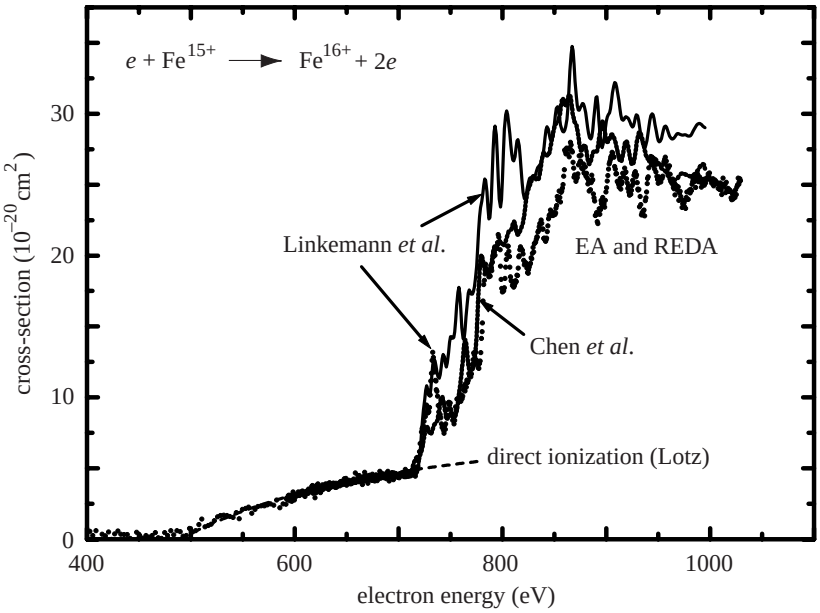

Figure 5. Cross-sections for electron-impact ionization of Fe^{15+} ions. The experimental data (Linkemann *et al*. 1995*b*) are indicated by solid dots. The solid and dotted lines are the results of extensive theoretical calculations from that same reference and of Chen *et al*. (1990). Direct ionization was estimated from the Lotz formula (Lotz 1968).

less, it has been possible to measure fine details in the ionization cross-sections of Li-like ions Si^{11+} and Cl^{14+} (Kenntner *et al*. 1995), as well as of Na-like ions Cl^{6+}, Fe^{15+} and Se^{23+} (Linkemann *et al*. 1995*a*, *b*). An example of the results obtained at the TSR in Heidelberg is shown in figure 5. The experimental cross-section for electron-impact net single ionization of Fe^{15+} ions is displayed together with two theoretical calculations. Above 750 eV, the cross-section is dominated by indirect processes (termed 'excitation autoionization' (EA) and 'resonant excitation double autoionization' (REDA)). Particularly remarkable is the wealth of resonance features, which are due to dielectronic capture (DC, see equation (3.4)) and subsequent emission of two electrons. While theory reproduces the overall size and structure of the measured cross-section, the fine details observed in the experiments are not matched by the calculations.

The experiments clearly show an increase in the importance of indirect ionization mechanisms relative to direct ionization mechanisms. While the contributions of EA and REDA are about the same as for the direct process in Cl^{6+}, the ratio of relative strengths moves towards 10 as one goes along the isoelectronic sequence to Se^{23+}.

(*b*) *Recombination*

(i) *The processes*

There are three fundamental mechanisms of recombination of A^{q+} ions with free electrons.

(1) Radiative recombination (RR):

$$\mathrm{e} + \mathrm{A}^{q+} \rightarrow \mathrm{A}^{(q-1)+} + h\nu, \tag{3.1}$$

where the excess energy released by the binding of an initially unbound electron is carried away by a photon in a direct process. After the RR process, the captured electron can be in a highly excited state and, hence, further radiation will be emitted until the electron is in its ground level.

The RR cross-section can be calculated using the semi-classical hydrogenic RR cross-section of Kramers (Kramers 1923; Bethe & Salpeter 1957), with some modifications

$$\sigma_{\mathrm{RR}}(E) = 2.1 \times 10^{-22}\ \mathrm{cm}^2 \sum_{n_{\min}}^{n_{\max}} k_n t_n \frac{(Z_{\mathrm{eff}}^2 R_\infty)^2}{nE(Z_{\mathrm{eff}} R_\infty + n^2 E)}. \tag{3.2}$$

In equation (3.2), the constants k_n are corrections to the semi-classical cross-section for low n (Andersen & Bolko 1990), and the constants t_n are weight factors accounting for already partly filled n shells. The minimum principal quantum number, $n_{\min}$, denotes the lowest electron shell with at least one vacancy. The effective charge can be assumed to be the ion charge and $R_\infty = 13.6\,\mathrm{eV}$ is the Rydberg energy. The maximum quantum number, $n_{\max}$, is determined by field ionization in the charge-state-analysing dipole magnet of the actual experiment. A formula for $n_{\max}$ that also accounts for higher n states that decay to below the field ionization limit on their way from the electron cooler to the dipole magnet is given in Müller & Wolf (1997):

$$n_{\max} = 1.846 Z_{\mathrm{eff}}^{4/5} ((\tau_{\mathrm{f}}/\mathrm{ns})\kappa(n_{\max})^2[-0.04 + \ln(n_{\max}) + \ln(\kappa(n_{\max}))])^{1/5}, \tag{3.3}$$

with $\kappa(n_{\max}) = 1.6 + 0.018 n_{\max}$, and τ_{f} the flight time of ions between electron cooler and beam-bending magnet (see figure 1).

(2) Dielectronic recombination (DR), where, in a first step,

$$\mathrm{e} + \mathrm{A}^{q+} \rightarrow [\mathrm{A}^{(q-1)+}]^{**}, \tag{3.4}$$

the excess energy released by the capture of the electron is absorbed within the ion by the excitation of a core electron; and where, in a second step, the intermediate multiply excited state decays by the emission of two or more photons

$$[\mathrm{A}^{(q-1)+}]^{**} \rightarrow [\mathrm{A}^{(q-1)+}] + h\nu_1 + h\nu_2. \tag{3.5}$$

The first step of the DR process, the dielectronic capture (DC, equation (3.4)), can only occur if the kinetic energy of the projectile electron matches the difference $E_{\mathrm{i}} - E_{\mathrm{f}}$ of total binding energies of all electrons in the initial and final states of the ion. The cross-section for DC can be expressed as

$$\sigma_{\mathrm{DC}}(E) = 7.88 \times 10^{-31}\ \mathrm{cm}^2\ \mathrm{eV}^2\ \mathrm{s}\ \frac{1}{E}\frac{g_f}{2g_i}\frac{A_{\mathrm{a}}(f \rightarrow i)\cdot \Gamma_f}{(E - E_{\mathrm{res}})^2 + \Gamma_f^2/4} \tag{3.6}$$

where g_f and g_i denote the statistical weights of the state $|f\rangle$ formed by DC and the initial state $|i\rangle$, respectively. $A_{\mathrm{a}}(f \rightarrow i)$ is the autoionization rate of

$|f\rangle$ for a transition to $|i\rangle$ and

$$\Gamma_f = h/(2\pi) \cdot \left(\sum_{j=1}^{n} A_\mathrm{r}(f \to j) + \sum_{j=1}^{n} A_\mathrm{a}(f \to j) \right), \tag{3.7}$$

the total width of $|f\rangle$ (h is Planck's constant).

The cross-section σ_DR for the whole process of DR, i.e. DC and subsequent relaxation by photon emission, is described by the product of σ_DC times the fluorescence yield ω_f of state $|f\rangle$, assuming an isolated DR resonance unperturbed by effects of interference with RR

$$\sigma_\mathrm{DR} = \sigma_\mathrm{DC}\omega_\mathrm{f}. \tag{3.8}$$

The fluorescence yield ω_f is given by

$$\omega_\mathrm{f} = \left(\sum_{j=1}^{n} A_\mathrm{r}(f \to j) \Big/ \Gamma_f \right) \frac{h}{2\pi}. \tag{3.9}$$

The sums in equations (3.7) and (3.9) extend over all radiative and Auger transitions from $|f\rangle$ to bound states $|j\rangle$, respectively. Further branching from states $|j\rangle$ would complicate the formulae considerably and is excluded here.

(3) Three-body (or ternary) recombination (TR)

$$\mathrm{e} + \mathrm{e} + \mathrm{A}^{q+} \to \mathrm{A}^{(q-1)+} + \mathrm{e}, \tag{3.10}$$

where one of the two electrons carries away the excess energy released by the recombination. TR, as a non-binary collision, becomes important only at high electron densities and low energies.

A widely accepted approach to TR is that provided by Mansbach & Keck (1969), extended by Beyer *et al*. (1989) to multiply charged ions by adding the Z^3 scaling. An approximate formula for calculating the associated recombination rate was derived:

$$\alpha_\mathrm{coll} = 2.0 \times 10^{-27}\ \mathrm{cm^6\ s^{-1}}\ Z^3 n_\mathrm{e} \left(\frac{\mathrm{eV}}{kT} \right)^{4.5}, \tag{3.11}$$

which is almost identical to a formula based on a paper by Thomson (1924), assuming that all Rydberg states with binding energies $E_n < kT$ are again destroyed by collisions. A spherically symmetric temperature distribution is assumed and no magnetic fields are included in the derivation of this equation.

None of the present experiments provides the electron densities and the electron temperatures for which TR to low lying bound levels of the recombined ions would be expected with measurable rates. TR into high Rydberg states is conceivable at low electron energies. However, the $\boldsymbol{v} \times \boldsymbol{B}$ motional electric fields ($\boldsymbol{v}$ is the ion velocity; $\boldsymbol{B}$ is the magnetic flux density) present in the experiments (e.g. in charge/mass analysing and storage-ring dipole magnets) strip off the Rydberg electrons of such states. And yet, some of the observations indicate a strong involvement of TR in the recombination rates measured at zero centre-of-mass energy $E_\mathrm{cm} = 0\ \mathrm{eV}$.

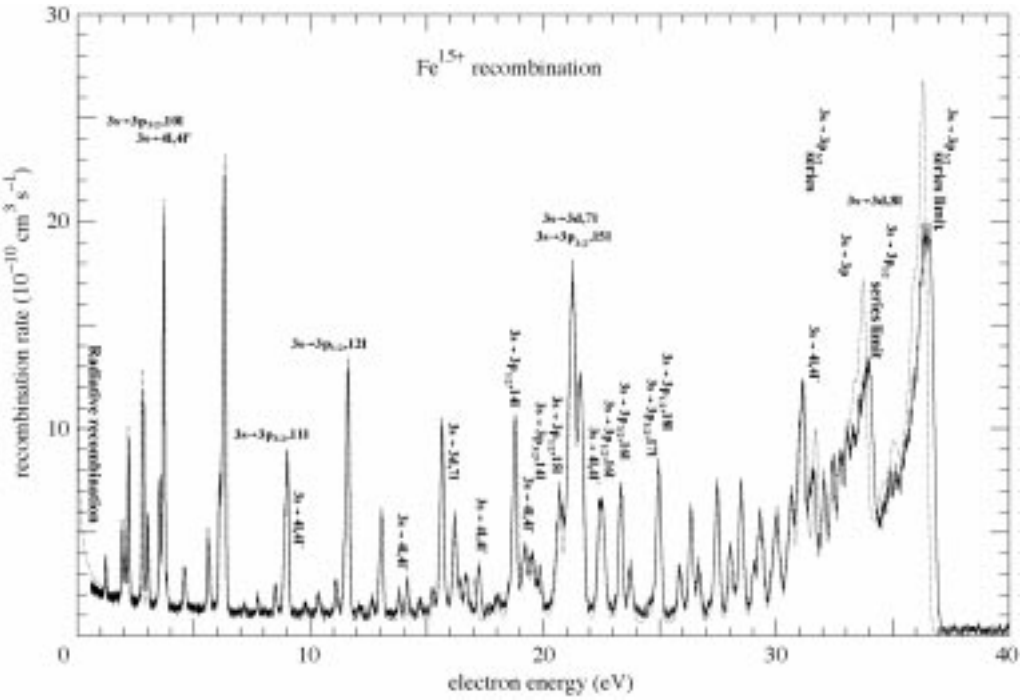

Figure 6. Measurements and calculations of recombination rates for Fe^{15+} ions (Linkemann *et al*. 1995*a*). The experimental data are indicated by the solid line. The dotted line is the result of the theoretical calculation.

(ii) *Plasma-relevant data*

Many of the plasma collision-data needs can be met by the application of heavy-ion storage rings. Particularly, recombination measurements with ions in intermediately high charge states are relatively straightforward. Most ions present in the solar corona or in a fusion plasma can easily be studied, for example, at the Heidelberg TSR.

An example of experimental recombination rates from the TSR is shown in figure 6. The process investigated here is DR of Fe^{15+} (Linkemann 1995*a*)

$$e + Fe^{15+}(2p^6 3s) \rightarrow Fe^{14+}(2p^6 n\ell n'\ell') \rightarrow Fe^{14+}(2p^6 3s^2) + \text{photons}. \qquad (3.12)$$

The 3s electron from the core of the parent ion is excited to a state with configuration $n\ell$, and the incident electron is captured into a subshell $n'\ell'$, with $n' = 3, 4, \ldots, \infty$. Subsequent to this DC process, the intermediate doubly excited state stabilizes the new charge state of the ion by the emission of photons. In the particular measurement displayed in figure 6, most of the transitions are related to $n = 3$. Few of the many resonances in the energy range of the figure are related to $n = 4$ (and $n' \geqslant 4$). Figure 6 includes theoretical calculations. Apart from discrepancies at the series limits of Rydberg resonance sequences, the agreement between theory and experiment is excellent.

The expected high quality of X-ray spectra from astrophysical objects to be obtained in future satellite experiments has led to a research programme at the TSR, in which recombination and ionization of the cosmically abundant ions Fe^{q+} with $q = 17, 18, \ldots, 23$ is studied. Recently, the measurement of the recombination

spectrum of fluorine-like Fe^{17+} ions provided a mild surprise for the astrophysics community (Savin *et al*. 1997). Different from previous expectations, the experiment showed the importance of M1 excitations of the $^2P_{3/2}$ core of Fe^{17+} ions in DR. Hence, in the cold plasma of X-ray-driven interstellar nebulae, the DR rate can be much higher (by two orders of magnitude) than previous calculations. Measurements with Fe^{18+} (Savin *et al*. 1999) and Fe^{19+} ions have recently been completed.

(iii) *Interference effects*

In particular cases, RR and DR cannot be distinguished by experiments, because initial and final states of the interaction process including the photons may be identical. This situation can lead to interference of the amplitudes for both pathways of the recombination process. Unified photorecombination theory predicts distortions of the DR resonance profiles as a result of such interference (Badnell & Pindzola 1992) and also for overlapping resonances of equal symmetry (Karasiov *et al*. 1992). An experimental observation of interference of RR and DR has been reported by Knapp *et al*. (1995) for differential cross-section measurements carried out at an ion trap.

Recent predictions by Gorczyca *et al*. (1997) suggested easy observability of interference effects in the recombination of argon-like Sc^{3+} ions through

$$\begin{array}{rcl} e^- + Sc^{3+}(3s^2 3p^6) & \rightarrow & Sc^{2+}(3s^2 3p^5 3d^2) \\ & \searrow \quad \downarrow & \\ & & Sc^{2+}(3s^2 3p^6 3d) + h\nu \end{array} \tag{3.13}$$

with the lowest excitation channels associated with $3p \rightarrow 3d$ and $3p \rightarrow 4s$ core transitions. In experiments at the TSR, an effort was made to measure recombination of these ions and to find interference effects (Schippers *et al*. 1998*a*, *b*). No clear-cut evidence for the predicted effects has been found so far. The experimental data for Sc^{3+} clearly show that the theoretical predictions have to be revised. A similar conclusion has to be drawn from a second measurement by Schippers *et al*. (1998*c*) with (isoelectronic) Ti^{4+} ions, which yielded much better statistics than the Sc^{3+} run.

(iv) *Influences of external fields on DR*

While electric fields were experimentally demonstrated to influence the size of DR cross-sections for singly charged ions (Müller *et al*. 1986), there were discrepancies between theory and experiment and inconsistencies in the understanding of these effects, particularly also for multiply charged ions. First quantitative measurements covering a wide range of controlled electric and magnetic fields have been carried out for Si^{11+} ions (Bartsch *et al*. 1997), showing that further detailed studies of field effects on DR will be necessary. Discrepancies with state-of-the-art theory sparked the prediction of a new mechanism of DR rate enhancement in the presence of an additional magnetic field perpendicular to the electric field (Robicheaux & Pindzola 1997; Robicheaux *et al*. 1998). Such magnetic fields have been involved in all but one of the previous DR measurements. Qualitatively, the assumption of additional m-mixing by magnetic fields on top of the ℓ-mixing caused by electric fields, and the resulting enhancement of DR cross-sections, is in accordance with the experimental observations. Clear-cut experimental proof of magnetic field effects in crossed $\boldsymbol{E}$ and $\boldsymbol{B}$ fields has been found recently (Bartsch *et al*. 1999).

(v) *Spectroscopy of high-Z ions*

The development of electron beams with increasingly better energy resolution, in connection with the bright cold ion beams available in the rings, has paved the way towards a precision spectroscopy of singly and multiply excited states of ions ranging from singly charged low-Z to very highly charged high-Z ions, where Z is the atomic number. With the resolution obtained in previous experiments, quantum electrodynamic (QED) effects on level energies could already be sensitively probed (Spies *et al*. 1995). A new step towards the best possible precision of energy determinations of excited states in very highly charged ions, and of Lamb shift measurements based on the observation of DR resonances, appears to be possible now (Brandau *et al*. 1998). Few-electron systems studied recently at the experimental storage ring ESR in Darmstadt comprise Li-like Au^{76+}, Pb^{79+}, Bi^{80+} and U^{89+} ions.

(vi) *Enhanced rates at low energies*

Unexpected high recombination rates at $E_{\rm rel} = 0$ eV were observed in merged-beams experiments with U^{28+} ions employing a cold dense electron target at the linear accelerator UNILAC of the GSI in Darmstadt (Müller *et al*. 1991). In an energy range between 0 and only about 1 meV, the observed recombination rate unexpectedly dropped by a factor of two from a huge maximum of almost 2×10^{-7} cm^3 s^{-1}, while a realistic estimate of the RR rate yields only a little over 1×10^{-9} cm^3 s^{-1}.

The experimental observations were surprising for two reasons. First, it had not been expected to find such a narrow feature in the measured rate spectrum, with electron-beam temperatures estimated to be $kT_{\|} = 1$ meV and $kT_{\perp} = 0.2$ eV at best. The analysis of DR peak shapes from the experiments rather suggests a transverse temperature corresponding to $kT_{\perp} = 0.5$ eV. Second, all estimates of RR rate coefficients under these conditions give much smaller numbers than those observed in the experiments.

It was immediately recognized that the lifetime of a stored cooled beam of U^{28+} ions would only be seconds, considering the electron density of an electron cooler, and yet this had not been widely noticed until after a series of experiments at the Low Energy Accumulator Ring (LEAR) at CERN, in which Pb^{53+} ions were stored and cooled in preparation for further acceleration (Baird *et al*. 1995). For $n_{\rm e} = 4.4 \times 10^7$ cm^{-3}, the beam lifetime was only 2 s, which is intolerable for efficient handling and acceleration of the ion beam. A similar phenomenon was recently observed with Bi^{64+} ions at the new cooler of the heavy ion synchrotron SIS in Darmstadt (L. Groening, personal communication).

While recombination rates for Pb^{53+} and Bi^{64+}, as well as their neighbour charge states, were determined only indirectly from lifetime measurements at LEAR and SIS, a special effort was recently made at the TSR (Uwira *et al*. 1997*a*) to investigate recombination of Au^{50+} ions, which are isoelectronic with Pb^{53+}. An extremely sharp peak was found at $E_{\rm rel} = 0$. Within approximately 4×10^{-4} eV, the recombination rate dropped from its maximum, which is as high as 1.8×10^{-6} cm^3 s^{-1}, to half this value. This is the highest recombination rate coefficient ever observed in merged-beams experiments. The enhancement factor beyond the expectation of RR theory is about 60. Apart from the recombination maximum at $E_{\rm rel} = 0$, huge DR peaks were detected. Already at $E_{\rm rel} = 30$ meV, a first resonance could be distinguished whose FWHM is only *ca*. 15 meV. The DR resonances are so densely spaced in energy

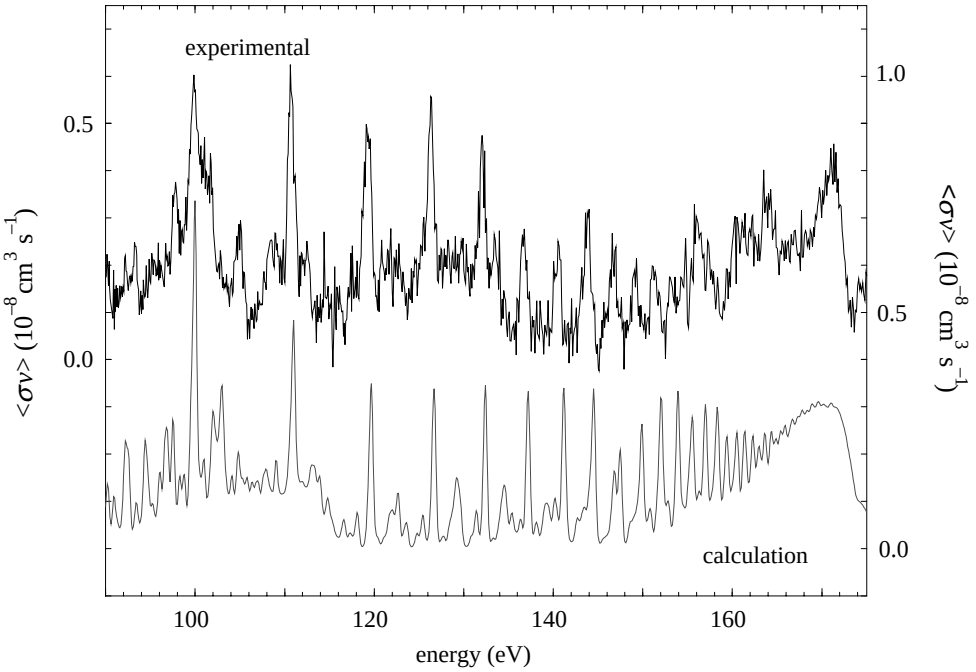

Figure 7. Recombination of U^{28+} ions with free electrons in the energy range 90–180 eV. The main features of the experimental results are well represented by the theoretical calculation (Mitnik *et al*. 1998). For clear presentation, the ordinate axis is shifted, the left axis corresponds to the experimental (upper) spectrum and the right axis to the theoretical (lower) spectrum.

that one can easily imagine strong resonance contributions also to the peak at zero energy. Apparently, excessive recombination enhancement beyond the expectations of RR theory is most likely due to DR resonances close to zero energy.

This can be demonstrated for the example of U^{28+} recombination. The early measurements that had been such a surprise were later repeated and extended to much higher relative energies (Uwira *et al*. 1995; Mitnik *et al*. 1998). In these experiments, a wealth of recombination resonances could be found extending up to several hundred electronvolts. Figure 7 gives a flavour of the density of DR resonances in the recombination spectrum of U^{28+} ions. In the figure, the experimental data are compared with a theoretical calculation (Mitnik *et al*. 1998).

It is quite likely that DR resonances also exist very close to the threshold, i.e. near zero relative energy. In this case, contributions of DR to the recombination rate at zero energy have to be expected. This is obvious already from the example presented in figure 3, where the convolution of a δ-resonance at 9 meV produces a finite rate at $E_{\mathrm{rel}} = 0$. The measured spectrum of U^{28+} does, indeed, show resonance structures down to the lowest energies. The resonance peaks, however, become almost indistinguishable below 1 eV, due to the temperatures of the electron beam in that experiment, which were $kT_{\perp} = 0.5$ eV and $kT_{\parallel} = 0.001$ eV. The radiative rate calculated from equation (3.2) using $Z_{\mathrm{eff}} = 28$, $n_{\mathrm{min}} = 5$, $t_5 = (50 - 4)/50$, $t_n = 1$ for $n \geqslant 6$ and $n_{\mathrm{max}} = 170$, is almost a factor of 200 below the experiment.

As a case study of recombination enhancement at low energies, an attempt was

made to simulate the observed recombination spectrum of U^{28+} assuming the presence of resonances at certain energies with certain resonance strengths of DR at low energies. The convolution of the DR cross-sections with the experimental velocity distribution produces substantial recombination at zero energy on top of pure RR. The following two resonances are artificially introduced: at $E_{\mathrm{res}} = 5 \times 10^{-4}$ eV, a δ-resonance (DR1) with a strength

$$S = \int \sigma(E)\,\mathrm{d}E = 8.8 \times 10^{-14}\ \mathrm{cm}^2\ \mathrm{eV};$$

and at $E_{\mathrm{res}} = 0.12$ eV, a Lorentzian-shaped resonance (DR2) with a width $\Gamma = 0.08$ eV and a strength $S = 6.7 \times 10^{-17}\ \mathrm{cm}^2$ eV. These two resonances are convoluted according to equations (2.2) and (2.3) with electron-beam temperatures $kT_{\perp} = 0.5$ eV and $kT_{\parallel} = 0.001$ eV. The resulting rate coefficient for DR1 is added to the RR rate calculated with equation (3.2) and displayed as the dashed line in figure 8. The RR contribution is of the order of only 1% of the sum and does not show up on the graph. DR2 produces the rate represented by the dotted line in figure 8, the sum of RR, DR1 and DR2 rate coefficients is given by the solid line. By introducing more resonances, it would clearly be possible to model the whole experimental spectrum in this way.

The strength of the resonance at 0.5 meV, which has to be assumed for the matching of calculation and experiment at the lowest energies, appears to be extraordinarily large. However, this number can be easily rationalized. The DR peak features at around 10 eV are already very large, containing resonance strengths of the order of $10^{-16}\ \mathrm{cm}^2$ eV. According to equations (3.8), (3.9) and most importantly (3.6), the DR cross-section is inversely proportional to the electron energy. When shifting a resonance with given width and fixed partial decay rates from higher to lower energy, equation (3.6) requires the resonance strength to increase with $1/E$. Hence, going from 10 eV down to 10^{-3} eV could easily lead to a resonance strength of $10^{-12}\ \mathrm{cm}^2$ eV, which is already a factor of 10 higher than necessary for explaining the present experiment near zero energy.

Despite the reasonable representation of the huge, narrow feature at $E_{\mathrm{rel}} = 0$ in U^{28+} by an assumed DR resonance represented by a δ-function, the enhancement phenomenon is not at all fully understood. Enhanced recombination at low energies is also found with completely stripped ions, which do not support DR (see, for example, Müller & Wolf 1997). Ever larger enhancement factors (up to about 10 for Ar^{18+}) have been observed for completely stripped ions in higher charge states (Gao *et al*. 1995, 1997; Uwira *et al*. 1996, 1997*b*). Besides DR fortuitously occurring around zero energy, there is, apparently, an additional, more fundamental, origin of enhanced recombination rates that has not yet really been found.

Systematic dependences of the enhancement on experimental parameters are presently measured at different experimental facilities. An example is an experiment with Au^{25+} ions at the high-density electron target where the U^{28+} data were also obtained. The data for Au^{25+} showed a record high enhancement factor of 365 of the measured recombination rate above theoretical expectations for RR (Hoffknecht *et al*. 1998). An increase in the electron density in the Au^{25+} experiment from $3.3 \times 10^8\ \mathrm{cm}^{-3}$ to $3.7 \times 10^9\ \mathrm{cm}^{-3}$ had no significant effect on the measured recombination rate, while the observed rate at $E_{\mathrm{rel}} = 0$ increased by more than a factor of two when the longitudinal magnetic field was tuned from 0.24 to 0.33 T.

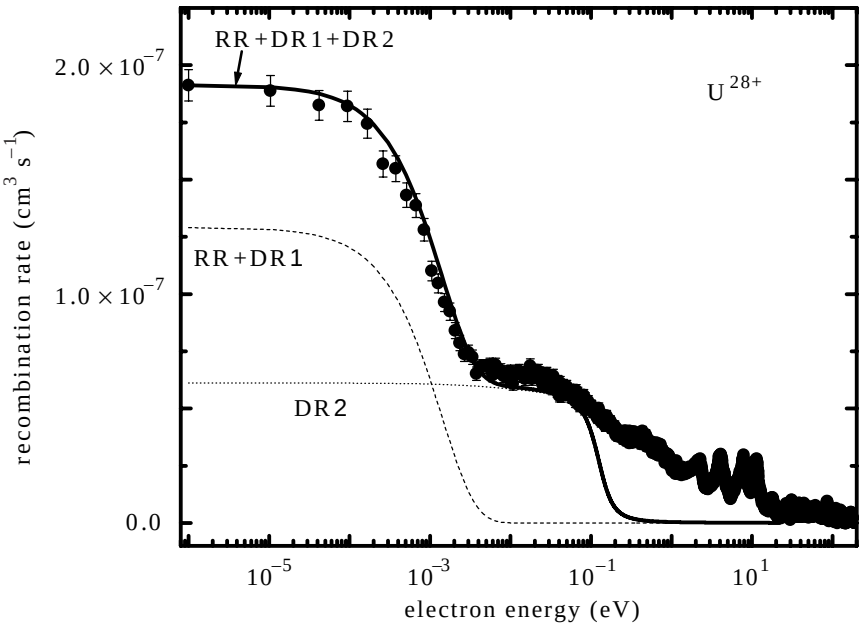

Figure 8. Recombination of U^{28+} ions with free electrons in the energy range 10^{-6}–2×10^{2} eV. The experimental data are those published by Mitnik *et al.* (1998). The figure includes the measured data displayed in figure 7. At energies below 20 eV, the experiment revealed recombination features exceeding the resonances of figure 7 by factors up to *ca.* 50. The recombination rate expected for RR is more than two orders of magnitude below these experimental data. For clarification of these observations, an attempt was made to represent the main features of the experiment by simulating the presence of DR resonances at the lowest energies. The assumed resonances are: a δ-resonance at 0.5 meV with a strength $S = 8.8 \times 10^{-14}$ cm^2 eV, and a Lorentzian-shaped resonance at 0.12 eV with a width $\Gamma = 0.08$ eV and a strength $S = 6.7 \times 10^{-17}$ cm^2 eV. The solid line gives the sum of the RR rate and the two convoluted DR resonances. The electron-beam temperatures used in the simulation are $kT_{\parallel} = 1$ meV and $kT_{\perp} = 0.5$ eV.

Collaboration between the author's group and colleagues at the ESR and the TSR led to measurements of a similar nature with variation of experimental parameters with Cl^{17+}, Au^{76+}, Pb^{79+}, Bi^{80+}, Bi^{82+}, Bi^{83+} and U^{89+} ions. Recombination rate enhancements are observed in all cases, although no DR resonances are expected for these ions at low energies (and are impossible for the completely stripped Cl^{17+} and Bi^{83+} ions). The results of that work are being analysed. Negligible effects of electron density variations in accordance with previous observations at CRYRING (Gao *et al.* 1997) seem to contradict the expectations based on molecular dynamics calculations (Zwicknagel *et al.* 1997) simulating the plasma conditions in the electron cooler.

4. Summary and outlook

Collisions of ions with free electrons lead to complex interactions. Due to their fundamental character, they provide an ideal testing ground for our understanding of atomic structures, transition probabilities and collision dynamics. In particular, DR can be employed for a collisional spectroscopy of multiply excited states. Extrapo-

lation of Rydberg resonance energies to their series limit can even provide precise excitation energies for singly excited states and, thus, opens new pathways towards high precision tests of QED calculations of energy levels in very highly charged few-electron systems. The physics of electron–ion recombination also involves unique and interesting phenomena, such as interference of different recombination channels or different, but overlapping, resonances of equal symmetry. The effects of external fields on DR provide an intriguing field for research. Surprising results are obtained at the very low relative energies that can now be accessed by the merged-beams technique, in storage rings using the cold electron beams of the cooling devices. At least for energies up to *ca.* 1 keV, the storage cooler rings provide the method of choice for studies of electron–ion recombination. These studies will be further extended in the near future. Electron-impact ionization studies at storage rings are more difficult. Only very few ion species will be studied using rings. The extension of the presently accessible electron–ion centre-of-mass energies is required for that. A big step in the potential and the quality of measurements will be possible when additional dedicated electron targets in the rings become available.

In conclusion, the theory for electron–ion interactions is already, and in the near future will be much more, challenged by the increasing experimental capabilities and precision of data measured at heavy-ion storage rings.

The author acknowledges very fruitful interaction with numerous colleagues and co-workers who have made possible the work to which this overview is related. Support by the Gesellschaft für Schwerionenforschung (GSI), Darmstadt; by the Max-Planck-Institut für Kernphysik, Heidelberg; by the German Ministry of Education, Science, Research and Technology (BMBF); and by the Human Capital and Mobility Programme of the European Community is acknowledged.

References

Andersen, L. H. & Bolko, J. 1990 *Phys. Rev* A **42**, 1184.

Andersen, L. H., Bolko, J. & Kvistgaard, P. 1990 *Phys. Rev.* A **41**, 1293.

Badnell, N. R. & Pindzola, M. S. 1992 *Phys. Rev.* A **45**, 2820.

Baird, S. (and 14 others) 1995 *Phys. Lett.* B **361**, 184.

Bartsch, T. (and 12 others) 1997 *Phys. Rev. Lett.* **79**, 2233.

Bartsch, T. (and 11 others) 1999 *Phys. Rev. Lett.* (In the press.)

Bethe, H. A. & Salpeter, E. E. 1957 Quantum mechanics of one- and two-electron systems. In *Handbuch der Physik* (ed. S. Flügge), vol. 35. Berlin: Springer.

Beyer, H. F., Liesen, D. & Guzman, O. 1989 *Part. Accel.* **24**, 163.

Brandau, C. (and 14 others) 1998 *Hyp. Int.* **114**, 49.

Brouillard, F. (ed.) 1986 *Atomic processes in electron–ion and ion–ion collisions.* New York and London: Plenum.

Chen, M. H., Reed, K. J. & Moores, D. L. 1990 *Phys. Rev. Lett.* **64**, 1350.

Dittner. P. F., Datz, S., Miller, P. D., Pepmiller, P. L. & Fou, C. M. 1987 *Phys. Rev.* A **35**, 3668.

Gao, H., DeWitt, D. R., Schuch, R., Zong, W., Asp, W. & Pajek, M. 1995 *Phys. Rev. Lett.* **75**, 4381.

Gao, H., Schuch, R., Zong, W., Justiniano, E., DeWitt, D. R., Lebius, H. & Spies, W. 1997 *J. Phys. Lett.* B **30**, 499.

Gorczyca, T. W., Pindzola, M. S., Robicheaux, F. & Badnell, N. R. 1997 *Phys. Rev.* A **56**, 4742.

Graham, W. G., Fritsch, W., Hahn, Y. & Tanis, J. H. (eds) 1992 *Recombination of atomic ions.* NATO ASI Series B: Physics, vol. 296. New York: Plenum.

Hoffknecht, A. (and 11 others) 1998 *J. Phys.* B **31**, 2415.

Karasiov, V. V., Labzowsky, L. N., Nefiodov, A. V. & Shabaev, V. M. 1992 *Phys. Lett.* A **161**, 453.

Kenntner, J. (and 10 others) 1995 *Nucl. Instrum. Meth. Phys. Res.* B **98**, 142.

Knapp, D. A., Beiersdorfer, P., Chen, M. H., Scofield, J. H. & Schneider, D. 1995 *Phys. Rev. Lett.* **74**, 54.

Kramers, H. A. 1923 *Phil. Mag.* **42**, 836.

Lampert, A., Wolf, A., Habs, D., Kenntner, J., Kilgus, G., Schwalm, D., Pindzola, M. S. & Badnell, N. R. 1996 *Phys. Rev.* A **53**, 1413.

Linkemann, J. (and 13 others) 1995*a* *Nucl. Instrum. Meth. Phys. Res.* B **98**, 154.

Linkemann, J., Müller, A., Kenntner, J., Habs, D., Schwalm, D., Wolf, A., Badnell, N. R. & Pindzola, M. S. 1995*b* *Phys. Rev. Lett.* **74**, 4173.

Lotz, W. 1968 *Z. Phys.* **216**, 241.

Mannervik, S., DeWitt, D., Engström, L., Lidberg, J., Lindroth, E., Schuch, R. & Zong, W. 1998 *Phys. Rev. Lett.* **81**, 313.

Mansbach, P. & Keck, J. 1969 *Phys. Rev.* **181**, 275.

Mitnik, D. M. (and 14 others) 1998 *Phys. Rev.* A **57**, 4365.

Müller, A. 1995 Dielectronic recombination and ionization in electron–ion collisions: data from merged-beams experiments. *Nucl. Fusion* (Suppl.) **6**, 59–100.

Müller, A. & Wolf, A. 1997 Heavy ion storage rings. In *Accelerator-based atomic physics techniques and applications* (ed. S. Shafroth & J. Austin), ch. 5, pp. 147–182. Woodbury, NY: American Institute of Physics.

Müller, A., Belić, D. S., De Paola, B. D., Djurić, N., Dunn, G. H., Mueller, D. W. & Timmer, C. 1986 *Phys. Rev. Lett.* **56**, 127.

Müller, A. (and 14 others) 1991 *Phys. Scripta* T **37**, 62.

Robicheaux, F. & Pindzola, M. S. 1997 *Phys. Rev. Lett.* **79**, 2237.

Robicheaux, F., Pindzola, M. S. & Griffin, D. C. 1998 *Phys. Rev. Lett.* **80**, 1402.

Savin, D. W., Bartsch, T., Chen, M. H., Kahn, S. M., Liedahl, D. A., Linkemann, J., Müller, A., Schmitt, M., Schwalm, D. & Wolf, A. 1997 *Astrophys. J. Lett.* **489**, 115.

Savin, D. W., Bartsch, T., Chen, M. H., Linkemann, J., Müller, A., Saghiri, A. A., Schippers, S., Schmitt, M. & Wolf, A. 1999 *Astrophys. J.* (Suppl.). (In the press.)

Schippers, S., Bartsch, T., Brandau, C., Linkemann, J., Müller, A., Saghiri, A. A. & Wolf, A. 1998*a* *Hyp. Int.* **114**, 273.

Schippers, S., Bartsch, T., Brandau, C., Müller, A., Linkemann, J., Saghiri, A. A. & Wolf, A. 1998*b* *Phys. Rev.* **59**, 3092.

Schippers, S., Bartsch, T., Brandau, C., Gwinner, G., Linkemann, J., Müller, A., Saghiri, A. A. & Wolf, A. 1998*c* *J. Phys.* B **31**, 4873.

Spies, W. (and 11 others) 1995 In *Proc. VIIth Int. Conf. on the Physics of Highly Charged Ions, Vienna, Austria, 19–23 September 1994. Nucl. Instrum. Meth. Phys. Res.* B **98**, 158.

Thomson, J. J. 1924 *Phil. Mag.* **47**, 337.

Uwira, O., Müller, A., Spies, W., Frank, A., Linkemann, J., Empacher, L., Mokler, P. H., Becker, R., Kleinod, M. & Ricz, S. 1995 *Nucl. Instrum. Meth. Phys. Res.* B **98**, 162.

Uwira, O. (and 15 others) 1996 *Hyp. Int.* **99**, 295.

Uwira, O. (and 14 others) 1997*a* *Hyp. Int.* **108**, 149.

Uwira, O. (and 13 others) 1997*b* *Hyp. Int.* **108**, 167.

Zwicknagel, G., Spreiter, Q. & Toepffer, C. 1997 *Hyp. Int.* **108**, 131.